Growth of disorder about point defects in a two-dimensional foam

A. Abd el Kader and J. C. Earnshaw*
Irish Centre for Colloid Science and Biomaterials,† The Department of Pure and Applied Physics, The Queen's University of Belfast, Belfast BT7 1NN, Northern Ireland
(Received 6 February 1998)

The evolution about isolated point defects of various kinds in two-dimensional liquid foam has been studied experimentally. As the foam about the defect coarsens it becomes disordered, the degree of disorder growing with time. This is broadly in line with recent simulations of defects in two-dimensional froths. The limitations on this comparison with theory are discussed. In the case of multiple dislocations in the foam the evolution leads ultimately to a decrease in disorder, which may be relevant to the changes found in the approach of relatively ordered soap froths to a scaling state. Tests of various topological correlations for the disordered foam about the defects suggest that it does not achieve statistical equilibrium during the experiments. [S1063-651X(98)05707-9]

PACS number(s): 82.70.Rr, 83.70.Hq

I. INTRODUCTION

The temporal evolution of two-dimensional soap froths has been the subject of much recent attention [1–3]. These cellular structures are of interest as models for the three-dimensional case, which is considerably harder to study both experimentally and theoretically. Foam is a nonequilibrium system which, in 2D, evolves under von Neumann's law. This relates the rate of change of the area of a cell (A) to the number of its neighbors (n, also referred to as its topological class):

$$\frac{dA}{dt} = k(n-6), \tag{1}$$

where k is a system-dependent constant. Previous work [3,4] has shown that relatively ordered soap froth exhibits an initial transient in its evolution to a final scaling state, which is independent of the initial state of the foam; this transient is absent for initially disordered foam. In a recent theoretical study, Levitan studied the growth of disorder due to a single defect in an otherwise ideal hexagonal froth [5]. His results suggested that the long-time topological distribution function, while of stable form, differed from that for generic initial conditions (random 2D froth). This excited some controversy [6,7], and stimulated subsequent computer simulations, which suggested that more conventional ideas are more likely correct [8–11]. This debate creates interest in the experimental investigation of the evolution of a single defect in an otherwise ideal 2D foam.

Most experimental studies of the evolution of 2D froths have involved bubbles confined between two closely spaced parallel glass plates [3,4]. However, it appears very difficult to create perfectly ordered foam in such an apparatus, making it difficult to carry out the studies of interest. However, Fortes *et al.* [12] have advocated bubble rafts on soap solutions as model 2D foams. By restricting such a bubble raft within a hexagonal cell, the required sixfold coordination of ideal 2D foams can be achieved [13]. It is possible to create various defects in the foam [13] to address the specific point at issue in the recent simulations: the behavior of an otherwise ideal 2D system containing a single defect.

In a previous paper [14], we reported such an experimental study for perfect 2D foam containing one bubble large enough to have more than six nearest neighbors. This study afforded qualitative support to the recent simulations [8]. However, various types of defect are possible and must contribute to the temporal evolution of the relatively ordered froths, including the initial transient [3]. It thus seems desirable to study the growth of disorder about all possible types of defect. The only other study of which we are aware involved, apart from the case of single large bubbles (with conclusions broadly similar to those of [14]), foams incorporating groups of larger or smaller bubbles [15]. While such groups may well exist in relatively ordered froths, there must also be point defects such as dislocations. Grain boundaries, which will also be present, form a special case and we defer their consideration to a future paper.

The present paper concerns an experimental investigation of the temporal evolution of ideally sixfold-coordinated 2D foams incorporating all possible types of point defect. The focus is largely on the topological properties of the area of disorder around the defect, as the metrical properties behave rather similarly to those for the isolated large bubbles previously considered [14]. We also consider briefly how the areas of disordered foam that develop about spatially separated defects interact with each other.

II. EXPERIMENTAL METHODS

The relevant simulations [5,8,9] all involve dry froth. As noted above, we use an adaptation of Bragg's bubble raft [16] to permit formation of perfectly ordered 2D foams. These foams are, of course, wet, but we hope that their behavior may reflect at least some of the generic aspects of the evolution of 2D froth. Our methods have been fully described elsewhere [13], and only an outline is needed here.

Bubble rafts trapped between a soap solution and a glass cover plate endure essentially indefinitely as diffusion of the

*Electronic address: j.earnshaw@qub.ac.uk
†Established at the Queen's University of Belfast and University College Dublin.

gas from the bubbles to the atmosphere is inhibited [12]. Temporal evolution is restricted to that due to coarsening of the bubbles, driven by differences in Laplace overpressure between bubbles of different radii. By forming such bubble rafts within a hexagonal cell, we enforce ordering of the 2D foam [13]. The glass cover is supported on top of this cell, 1–3 mm above the soap solution. The 2D foam is formed by bubbling N_2 into the solution below the cell via a long hypodermic needle. The bubbles are attracted to the cell wall and to each other by comparatively long-ranged capillary forces [17]. It is possible, with practice, to create within a hexagonal cell 6 cm on a side, as used in the present work, a perfectly sixfold-coordinated lattice comprising ≈ 3000 bubbles about 2 mm in diameter. While there must be minor variations in bubble diameter within a given lattice, these are not large enough to affect the regularity of packing to any noticeable degree.

We follow the growth of disorder in the system induced by introducing one or more defects into such 2D foam [14]. The defect is introduced by interrupting the process when the foam is half made, forming the defect, and then completing the regular foam around it. Different types of defect require different techniques for their creation [13].

(i) A dislocation is created by part filling the cell with an ideal lattice, then making two portions of lattice separated by a narrow channel but in register with the initial partial lattice. The channel fills in as the cell is subsequently filled with bubbles, spontaneously forming the dislocation [13].

(ii) Impurity bubbles comprise isolated bubbles of different size from those forming the foam. We define topological defects here as large impurity bubbles having more than six nearest neighbors (such other point defects as dislocations are of course topological defects, but we restrict our usage of the term to that just defined). Impurity bubbles cross over to topological defects when the bubble is about 40% larger in diameter than the lattice bubbles [13]. All these defects are formed by injecting an isolated bubble of different size to those forming the 2D foam, and then completing the lattice around it.

(iii) Both vacancies and bound pairs of dislocations are created in two stages. The first stage is to create a 2D lattice with a single dislocation. The second stage involves adding bubbles into one of the missing half layers of bubbles forming the dislocation. If one less bubble is added than the number required to complete the extra half layer, a vacancy is introduced; if one more than this number, a bound pair of dislocations is created. A dislocation involves neighboring fivefold- and sevenfold-coordinated bubbles. A bound pair of dislocations thus involves two fivefold- and two sevenfold-coordinated bubbles. This defect differs from the bound pair of dislocations that results from an elementary T_1 process [1] in an ideally sixfold-coordinated foam. In the latter case the two sevenfold-coordinated cells must be adjacent. Using our methods it seems impossible to achieve this; rather it is the two bubbles with five neighbors that are initially adjacent.

III. RESULTS AND DISCUSSION

In this study we present data from a series of experiments with a hexagonal cell of side 6 cm. These experiments encompass the evolution of the various point defects in an otherwise regular hexagonal foam. Before presenting our results, we consider some points that are generally relevant.

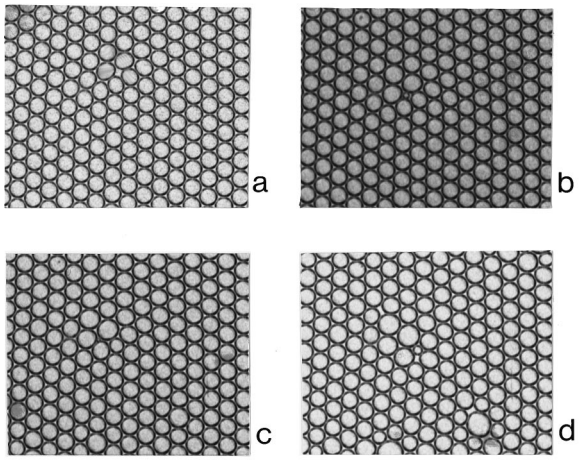

FIG. 1. Pictures of a typical evolving foam containing a dislocation. (a) As formed ($t=0$) and after (b) $t=10$, (c) $t=15$, and (d) $t=20$ h.

Except for vacancies, which cannot occur in soap froths, we compare our data with the results of recent computer simulations [2,5,9]. We defer detailed discussion of various limitations on these comparisons to Sec. IV. We follow Jiang *et al.* [8] and our previous paper [14] in studying the evolution of that set of bubbles around the initial point defect having at least one nonhexagonal neighbor (called ''the cluster''). However, foams containing an impurity bubble are initially entirely sixfold coordinated, so we define the cluster in this case as the first shell of bubbles around the impurity plus the impurity bubble itself.

This definition of the cluster is somewhat arbitrary. However, an alternative definition [9], excluding the outer belt of sixfold-coordinated bubbles, leads to distributions of topological classes, $P(n)$, which are not unimodal, and for which the statistics of interest are subject to greater fluctuations. The arbitrary nature of the cluster implies that the absolute values of these statistics may not be very significant; we therefore focus principally upon their temporal evolution.

As time progresses, the disorder increases due to coarsening, the first observable changes occurring after 10–13 h (Fig. 1). At early stages, the disorder is localized round the initial defect, propagating outwards with time. As pointed out by Jiang *et al.* [8], three distinct topological regions may be identified at any instant around a defect: the ''core'' of the defect (for example, the isolated large bubble in the case of the topological defect), a ''boundary'' of cells having at least one neighbor that is not sixfold-coordinated, and the remainder of the foam, unaffected by the defect. In simulations a cell within the latter region will remain ideally sixfold-coordinated until the disorder around the defect penetrates to it. In our experiments, however, inevitable tiny differences in the size of the ''ordered'' bubbles in the body of the foam lead to coarsening, so that generalized disorder appears over time scales of the order of days. This limits the time over which we can follow the changes due to the defect, as eventually the growing cluster meets this generalized disorder. All the data presented here relate to times before this occurred. At late times in some experiments the behavior de-

parts from the trend evident at earlier times, perhaps due to the generalized disorder affecting the local packing around the cluster in such a way that the cluster can grow unusually fast towards this different region of foam. This feature does not seem to perturb any of the present data.

In the simulations time (t) could be used as an independent variable [8,9]. However, as we will see, experimental factors can influence the time evolution of the foam. The size of the cluster increases with time, both experimentally [14] and in simulations [8], and so it seems reasonable to use the number of bubbles in the cluster (n_c) as the independent variable, instead of time itself. We do not claim that n_c depends linearly on t (although in simulations this is found to be the case for at least certain types of defect [8]), just that it provides a measure of the evolution of time in the system.

Experimentally, n_c grows with time, as does the number of bubbles adjoining the initial large bubble (n_b) for foams containing large bubbles. In that case the two quantities are related [14], supporting the conclusion of the simulations [8] that the outward propagation of the disorder in the foam just follows the growth of the impurity bubble. This reflects the fact that the boundary is usually only some two bubbles wide (see Fig. 4 below), as found in the simulations [8]. While n_c generally seems to be a smooth function of n_b, towards the end of an experiment n_c may increase relative to the general trend [14]. As noted above, this may occur as the cluster approaches the regions of generalized disorder, although we cannot presently confirm this.

The two basic topological transformations in foam (T_1, neighborhood switching, and T_2, cell disappearance [1]) underlie the temporal behavior described here. In particular, for certain types of defect unique patterns in the early stages of evolution can be understood in terms of distinct sequences of T_1 processes. In such regimes the distribution of topological classes in the cluster is deterministic, and so its moments are exact. T_2 processes tend to occur more reluctantly than in 2D soap froths, due to the very small surface area of the threefold-coordinated bubbles, which are tiny compared to those bubbles comprising the body of the foam.

We should note another complication of our wet foams: the plateau borders between the bubbles can lose their triangular shape, multiple borders forming as threefold borders merge [18]. Such multiple borders potentially lead to some ambiguity concerning adjacency of bubbles, but in practice this can always be resolved unambiguously.

A. General development and topological class distribution

1. Dislocations

For dislocations we distinguish between two types. For one, the initial changes in the foam after 10–13 h involve growth of disorder around the 5/7-coordinated pair of bubbles constituting the dislocation [Fig. 1(b)]. However, for the other the first change (after a similar time) involves the creation of one or two new dislocations elsewhere in the foam, followed by the growth of disorder around the original dislocation. In the latter case, we studied only the evolution of disorder about the original defect; that about the new dislocations was generally similar. After the different initial behaviors the topological evolution for both cases was broadly the same. We show their data together for ease of comparison.

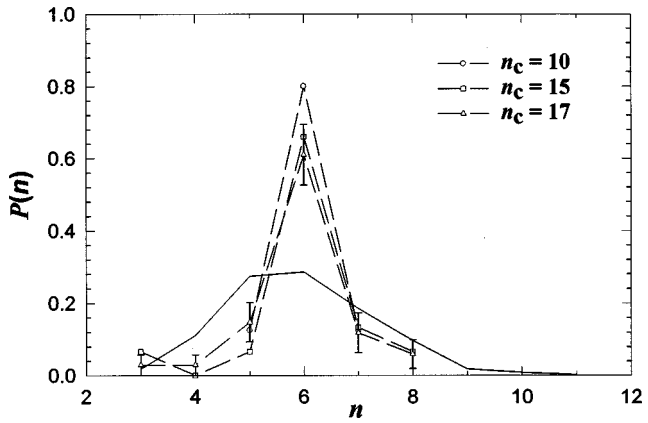

FIG. 2. Topological class distributions $P(n)$ for an evolving foam containing a dislocation; values of n_c as in the legend. The full line indicates $P(n)$ for a random cellular structure (see text).

The second type of behavior was usually observed when the bubbles were less compactly packed than for the first case. This allowed the bubbles to relax with time, and a line of bubbles ending close to a corner of the hexagonal cell could slide relative to this corner (perhaps due to the stress field of the dislocation) to form two extra half-layers of bubbles.

Figure 2 shows the topological class distribution, $P(n)$, of the cluster about a dislocation, and its evolution. $P(n)$ peaks at $n=6$; as the cluster ages $P(6)$ falls and $P(n)$ gets wider. As sixfold-coordinated cells can be regarded as ''ordered,'' $P(6)$ is a measure of order whereas the width of $P(n)$ (quantified via its second central moment, μ_2) is a measure of disorder. The decrease in $P(6)$ and the widening of $P(n)$ thus indicate that the cluster is becoming more disordered with time.

These $P(n)$—which are broadly typical of those in all our experiments—are rather different from those reported for many 2D cellular networks, as illustrated by comparison with $P(n)$ for a Voronoi network based on 1000 points randomly distributed in a plane (Fig. 2). In our foam, $P(6)$ remains comparatively high, while the populations of threefold-coordinated bubbles and at larger n quickly become relatively large. Such a population at $n=3$ is unusual; in conventional 2D froths such bubbles disappear through the T_2 process [1], leaving a rather small $P(3)$. In the present foam the threefold-coordinated bubbles are small, and they tend to lie around large bubbles. The difference from 2D froths clearly lies in the wetness of our foams. The area of contact available for diffusive interchange of N_2 between the smallest bubbles and their neighbors falls more rapidly (area $\propto r^2$) for the present quasispherical bubbles than in 2D froths (where a threefold-coordinated cell forms a triangular prism; area $\propto r$), hindering the final stages of evolution leading to the T_2 process.

Figure 3 shows the temporal evolution of μ_2. This statistic is initially 0.20, as the cluster comprises eight sixfold-coordinated bubbles and a single fivefold- and sevenfold-coordinated pair. It increases deterministically as the 5,7 pair changes to one fourfold- and two sevenfold-coordinated

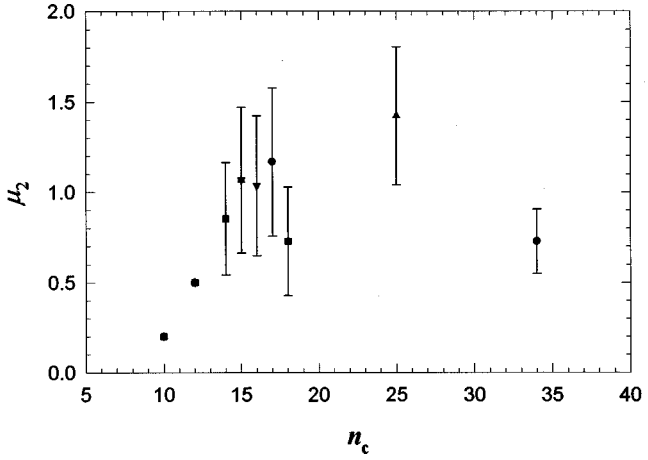

FIG. 3. Variation of μ_2, the second moment of the cluster with n_c as different foams (different symbols) containing a dislocation evolve.

bubbles (Fig. 1) and then increases less predictably to reach a value ≈ 1.4 but eventually starts to decline. While the second type of dislocation evolves faster than the first, the behavior of μ_2 with n_c is basically the same (similar values of μ_2 are reached at large n_c in both cases).

2. Impurity bubbles

Figure 4 shows the typical evolution of an impurity bubble. The second moment of $P(n)$ starts at zero, as initially all bubbles in the cluster are sixfold-coordinated, and increases with n_c to quite large values, but may ultimately decline [Fig. 5(a)]. The large values of μ_2 are basically due to the impurity bubble itself ($n=n_b$) and so may not be characteristic of the disorder induced in the foam by the defect. Restricting ourselves to the boundary of the cluster (as defined by Jiang *et al.* [8]: the cluster minus the large bubble) yields more representative results [Fig. 5(b)]. The second moment for this case (μ_2') increases to a lower value than that for the whole cluster, and again may later decline somewhat.

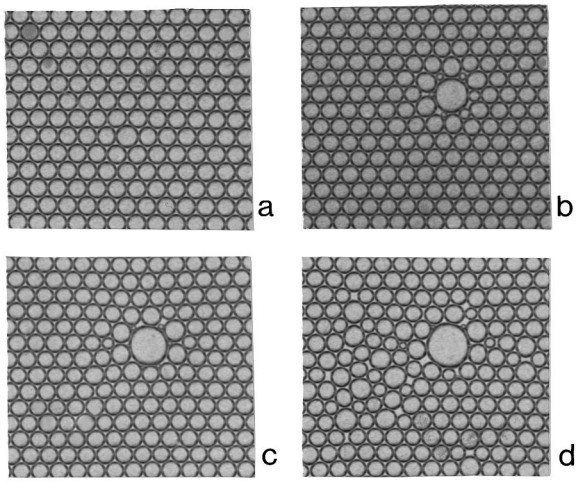

FIG. 4. Pictures of a typical evolving foam that contains an initial isolated larger bubble, constituting an impurity defect for (a) $t=0$, (b) 19, (c) 32, and (d) 43 h.

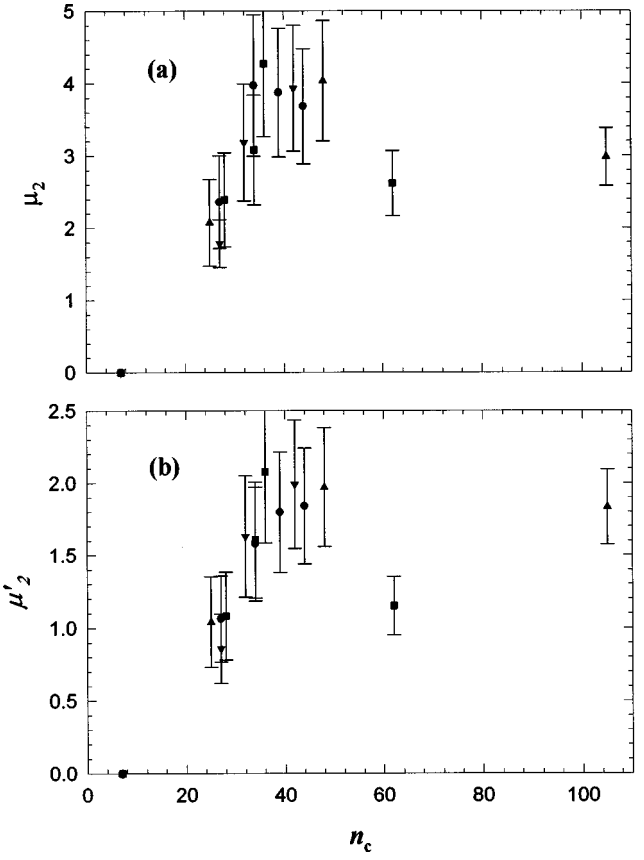

FIG. 5. (a) Variation of μ_2 with n_c for foams containing an impurity. (b) Evolution of μ_2', the second moment of the cluster boundary. The initial values of μ_2 and μ_2' are zero.

Such impurity bubbles resemble, in part, the topological defects defined above. We have previously reported the evolution of foams containing such topological defects having n_b from 8 to 16 [14]. These data were somewhat inconclusive in that, as just noted for impurity bubbles, the long-time behavior of μ_2' might or might not have involved a slight decrease. We have, therefore, investigated the behavior of topological defects for large n_b (19 or 20) to probe the long time limit more conclusively. The second moment of the cluster μ_2 increases with n_c reaching rather large values [Fig. 6(a)], as found in the earlier experiments [14,15] and in simulations [8]. However, it then clearly falls, forming a peak. Similarly μ_2' grows to a value of about 2 before declining [Fig. 6(b)].

The clearer peaks in μ_2 and μ_2' for foams containing topological defects with $n_b=19$ or 20 are due to the higher rate of gas diffusion between the large central bubble and its neighbors, reflected in von Neumann's law [Eq. (1)]. Some of the neighboring bubbles become very small in a relatively short time, and thus have time to disappear before the cutoff due to the generalized disorder. The slower evolution for lower n_b makes such decisive experiments more difficult.

These peaks in μ_2 and μ_2' do not appear in simulations, where both statistics increase more or less steadily with time [8,9]. We relate the observed decline of μ_2 and μ_2' to the delay to late times of the disappearance of threefold-coordinated bubbles around the initial large bubble; it is, therefore, not surprising to find such discrepancies from the

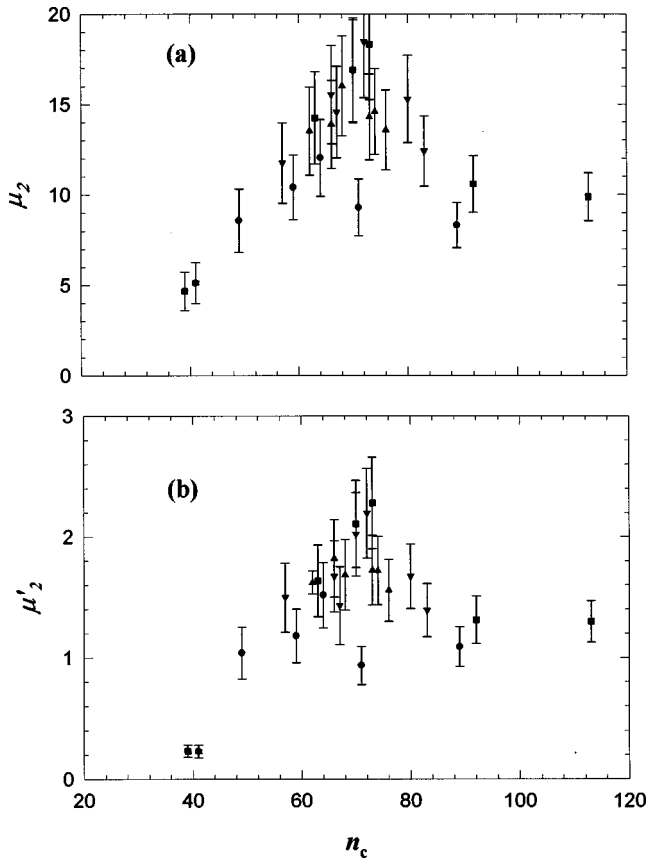

FIG. 6. As Fig. 5, for large topological defects.

simulation results (T_2 processes occur easier in froths and so will be more randomly distributed in time). This point is significant, as it implies that the decreases in μ_2 and μ_2' that we observe are not related to that in the transient found by Stavans and Glazier for relatively ordered foam [3].

The above data relate to impurity bubbles larger than those forming the foam. We have also studied impurity bubbles smaller than those comprising the lattice. In this case, while the impurity bubble shrinks rather than growing, μ_2 follows a trend much as for larger bubbles. However, it does not reach as high a value as in that case [Fig. 5(a)], as seems reasonable given that those high values are due to the large n_b. However, over the limited range of n_c the data are consistent with those for larger impurities.

3. Pair of dislocations

Turning to the bound pair of dislocations, the early development of the cluster (Fig. 7) follows a clear deterministic sequence of T_1 processes. The initial cluster has two fivefold-, two sevenfold-, and twelve sixfold-coordinated bubbles. The first change involves the fivefold-coordinated bubbles becoming fourfold-coordinated and the sevenfold-coordinated bubbles becoming eightfold-coordinated. This is followed by two simultaneous T_1 processes, the fourfold- and eightfold-coordinated bubbles becoming, respectively, threefold- and ninefold-coordinated, while two pairs of fivefold- and sevenfold-coordinated cells appear. Thereafter, the evolution of the system is no longer deterministic.

The second moment μ_2 grows monotonically from 0.286 (Fig. 8). The initial increase occurs without change in n_c.

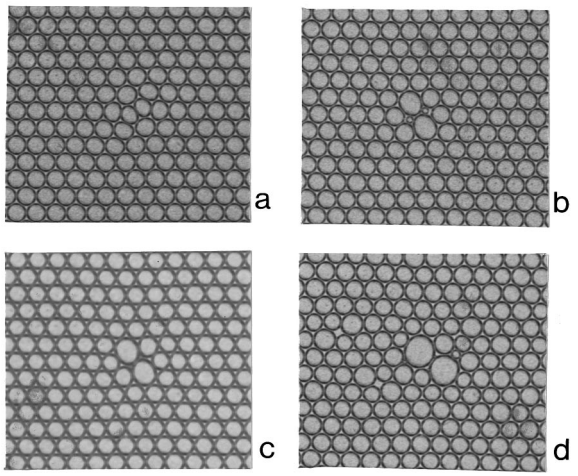

FIG. 7. Pictures of a foam containing a bound pair of dislocations. (a) The initial state ($t=0$) and after (b) $t=20$, (c) $t=27$, and (d) $t=35$ h.

Ultimately μ_2 appears to increase roughly linearly with n_c. This broadly agrees with the results of simulations of the evolution of foam containing a single defect formed by an elementary T_1 process [9]. The difference in the initial state between our experiment and that of the simulations (experimentally fivefold-coordinated cells are adjacent, after T_1 the sevenfold-coordinated cells are) appears not to affect the development of μ_2.

4. Vacancy

For the vacancy (Fig. 9), the initial cluster has 18 bubbles (six fivefold-coordinated surrounding the actual vacancy, and twelve sixfold-coordinated: $\mu_2=0.22$). The vacancy first collapses as the bubbles around it grow, leading to one of two different topological arrangements in the cluster (three fivefold-, three sevenfold-, and twelve sixfold-coordinated or two fivefold-, two sevenfold-, and twelve sixfold-coordinated). In the first case, $P(6)$ stays the same while μ_2 increases to 0.33, while for the other, $P(6)$ increases because n_c falls and μ_2 increases to only 0.25. [This indicates the approximate nature of $P(6)$ and μ_2 as measures of order and disorder. While these two statistics are usually inversely cor-

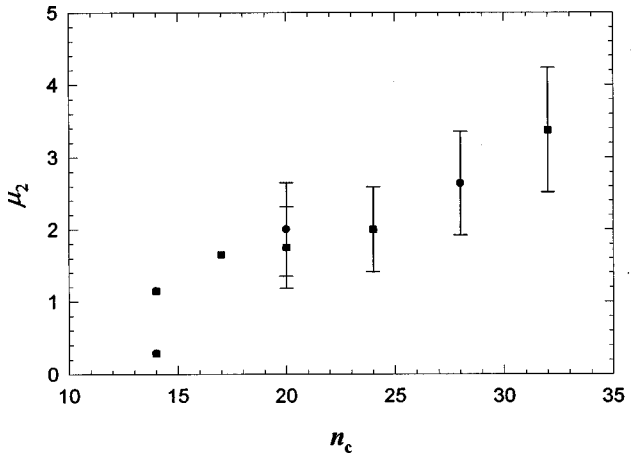

FIG. 8. The variation of μ_2 with n_c for bound pairs of dislocations.

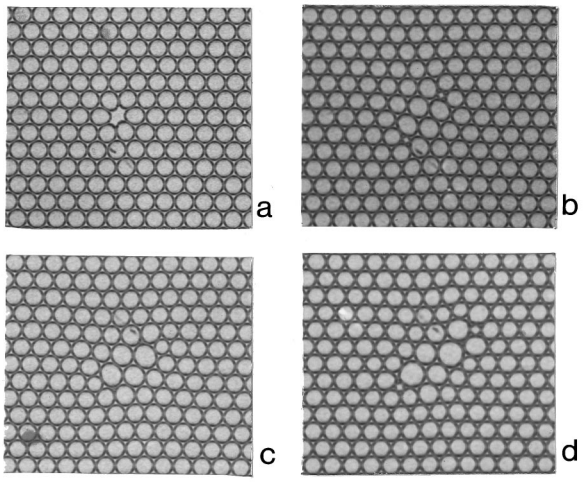

FIG. 9. A typical evolving foam with a vacancy at (a) $t=0$, (b) $t=16$, (c) $t=23$, and (d) $t=33$ h.

related, special cases may show the opposite tendency.] Subsequently μ_2 grows monotonically with n_c to quite high values for both cases (Fig. 10).

One set of data in Fig. 10 represents an experiment in which the surface of the solution was in contact with the glass covering the hexagonal cell, rather than leaving a gap, removing the capillary attraction between the bubbles [13]. This delayed the evolution of the foam by about 12 h, after which time the data paralleled those for other foams containing a vacancy. However, all the data collapse on a common variation when plotted against n_c. It is such experimental effects that lead us to use n_c as a measure of time.

B. Topological correlations

For cellular structures it is known that adjoining cells are correlated: few-sided cells have many-sided neighbors and vice versa [1]. We therefore now turn to various topological correlations in the clusters.

According to the Aboav-Weaire law [19,20], a widely obeyed semiempirical formula, for finite networks the mean number of sides of cells adjoining an n-sided cell is [21]

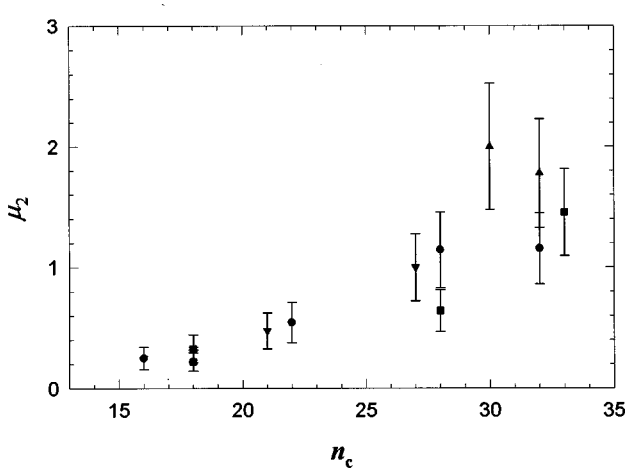

FIG. 10. Variation of μ_2 with n_c for foams with a vacancy (see text for discussion).

$$m(n)=\langle n\rangle-a+\frac{\langle nm(n)\rangle-\langle n\rangle^2+\langle n\rangle a}{n}. \tag{2}$$

This law embodies two relations, the semiempirical Aboav's law [19]

$$m(n)=A+\frac{B}{n}, \tag{3}$$

and Weaire's rigorous sum rule [22]

$$\langle nm(n)\rangle=\langle n\rangle^2+\mu_2. \tag{4}$$

For infinite networks Euler's rule implies $\langle n\rangle=6$ and the Aboav-Weaire law reduces to the form usually quoted:

$$m(n)=6-a+\frac{6a+\mu_2}{n}. \tag{5}$$

Aboav's law can be derived from arguments based on maximum entropy [23], and hence may represent an expression that a cellular structure obeying it is in statistical equilibrium. While the parameter a is generally found to be ≈ 1, these arguments do not predict its value. We note, however, that the Aboav-Weaire law involves a in both the intercept and gradient of the linear dependence of $m(n)$ upon n [19], permitting a check upon consistency of the data.

For a finite network of N cells Euler's rule becomes [24]

$$\langle n\rangle\leqslant 6-\frac{12}{N}. \tag{6}$$

All our data for the evolved clusters obey this relation, using n_c for N (certain initial states do not obey Euler's rule). The data also all agree with Weaire's sum rule to within 1%.

Now $m(n)$ does not vary much with n, so that the common practice of plotting $nm(n)$ versus n can conceal deviations from the law [Weaire (private communication)]. It is preferable to test the form of the law by plotting $m(n)$ versus n^{-1}. This is done in Fig. 11 for the various point defects. For clarity only one state of foam for each type of point defect is shown, usually that at largest n_c (time) as the cluster must then have evolved some way towards equilibrium. While individual cases are probably not statistically significant, the same trends were always observed for the different types of defect, suggesting that the variations shown are indeed representative.

Dislocations and vacancies yield linear relationships [Figs. 11(a) and 11(b)]. In both cases values of a derived from the slope and intercept of a linear fit are mutually consistent (Table I), enabling us to claim agreement with the Aboav-Weaire law. The values of a are, however, different in the two cases. This, and the differences from unity of the estimates of a for the vacancy, is not surprising, as only for foams dominated by T_2 processes or cell division (impossible here) should $a=1$ [Rivier (private communication)].

However, the bound pair of dislocations and impurity bubbles (both large and small, and including topological defects) consistently gives nonlinear plots [Figs. 11(c) and 11(d)]. We initially associated these departures from linearity with the tiny threefold-coordinated bubbles. However, even when we ignore the presence of such bubbles, the plots

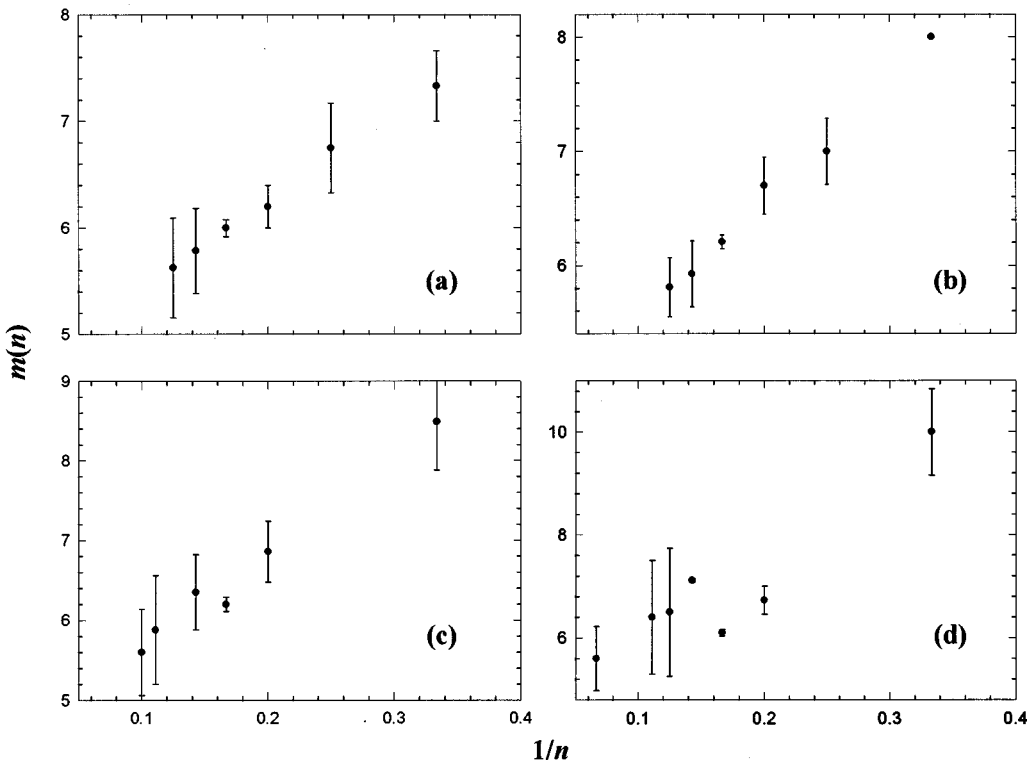

FIG. 11. The n dependence of the average number of sides of cells neighboring an n-sided cell in clusters about single defects: (a) dislocation, (b) vacancy, (c) bound pair of dislocations, and (d) impurity.

retain the same general form. In both cases there are large bubbles ($n \geqslant 7$) in contact with each other: the correlations are not as described by the Aboav-Weaire law. This positive association of large bubbles with each other causes $m(n \geqslant 7)$ to be larger than expected from the trend for lower n. For dislocations and vacancies the evolution evidently does not lead to such associations.

The disagreements with the Aboav-Weaire law, which we find in some cases, are not really surprising—our foams evolve over relatively short periods of time from specific initial conditions, and so might well not be expected to be in statistical equilibrium. The high values of $P(6)$ typical of our data indicate that the clusters are rather ordered structures, even in their final stages. Indeed, from this point of view the linear Aboav-Weaire plots found for dislocations and vacancies are rather surprising. Now linear Aboav-Weaire plots need not imply equilibrium [21]; unfortunately the statistics of our clusters are not adequate to test the maximum entropy origin of those linear Aboav-Weaire laws that we do find. Departures from linearity are expected for polydisperse distributions of cells [25] and the great differences in size between bubbles with $n=3$ or $\geqslant 6$ may underlie some of the deviations seen in Figs. 11(c) and 11(d).

As the clusters which evolve about defects are still rather ordered structures, we investigated a sample area (of 260 bubbles) randomly chosen from the whole foam at a late time, when it appeared generally very disordered. For this sample $P(n)$ is much more consistent with literature data for soap froths [3] and the Aboav-Weaire law is smooth and linear (Fig. 12). The values of a are again mutually consistent (Table I).

In earlier studies of topological correlations of random 2D cellular structures it has been found that μ_2 varies with $P(6)$ in an apparently universal manner [21,26]. According to Lemaître *et al.* [26] this relation is the equivalent, for such random structures, of the virial equation of state in statistical mechanics [27]. Remarkably the virial coefficients do not vary from case to case: data for a very wide range of 2D mosaics collapse onto a universal curve, implying that the various $P(n)$ examined belong to a specific universality class [26]. The universal curve can be parametrized as [21]

$$\mu_2 P(6)^2 = 0.150 \pm 0.014, \tag{7}$$

the so-called Lemaître law.

TABLE I. Computation of values of a from the intercept (a_c) and slope (a_m) for the linear Aboav-Weaire plots of Figs. 11 and 12.

Defect type	slope	intercept	μ_2	$\langle n \rangle$	a_m	a_c
dislocation	7.95 ± 0.39	4.69 ± 0.08	1.16 ± 0.41	5.86 ± 0.26	1.16 ± 0.11	1.17 ± 0.28
vacancy	10.50 ± 0.49	4.48 ± 0.11	1.16 ± 0.29	5.98 ± 0.19	1.56 ± 0.11	1.50 ± 0.22
disordered	6.69 ± 0.13	5.30 ± 0.02	2.92 ± 0.10	5.98 ± 0.04	0.63 ± 0.06	0.69 ± 0.05

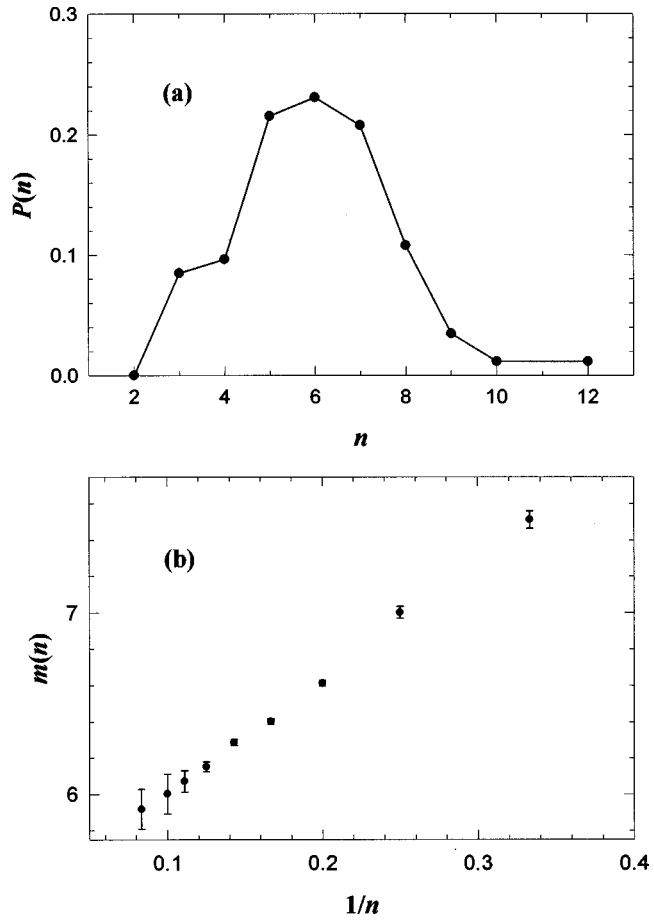

FIG. 12. (a) The topological class distribution and (b) the Aboav-Weaire plot for a sample of very disordered foam.

Figure 13 shows the relationship between μ_2 and $P(6)$ for all types of defects that we have studied: the data represent the evolution of a single cluster for each type of defect. While these data appear to collapse reasonably well onto a common trend (within rather large uncertainties), the value of μ_2 for a given $P(6)$ is much larger than given by Lemaître's law. The difference is not surprising as the threefold-coordinated bubbles make our values of μ_2 high, while $P(6)$ retains a high value. As noted above, the clusters are really rather well ordered, even in the final stages. It is rather remarkable that states of our system arising from different initial conditions collapse tolerably well onto a common form: the initial state has rather little impact. Indeed, measurements of the areas of generalized disorder, which evolve in the initially ordered region of foam, yield values of μ_2 and $P(6)$ that accord well with the trends shown in Fig. 13.

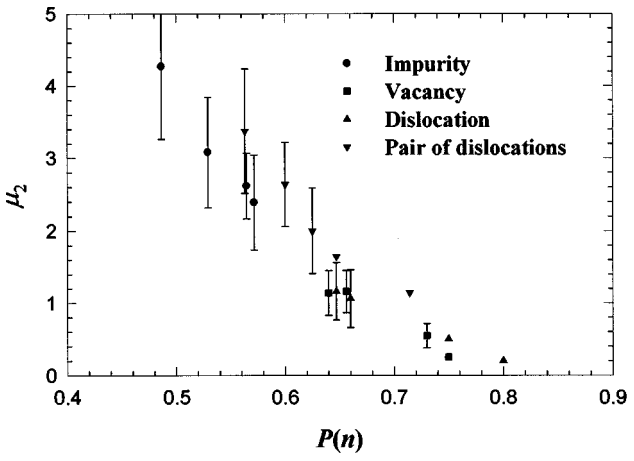

FIG. 13. Plot of μ_2 against $P(6)$ for the various point defects.

As noted above, the large values of μ_2 in the present study arise from threefold-coordinated bubbles, which here persist rather than disappearing through T_2 processes randomly occurring in time. Our foams are, in this sense, always comparatively young. For the sample of 260 bubbles in the final stages of evolution of the foam, when it appears generally very disordered, $P(n)$ (Fig. 12) is very different from those found for the clusters about the defects (Fig. 2). These data yield $P(6)=0.23\pm0.03$ and $\mu_2=2.92\pm0.10$, in excellent accord with Lemaître's law [21].

As a virial equation, the Lemaître law can only be valid for foam in equilibrium. It is thus not entirely surprising that our clusters do not obey it. This further reinforces the suggestion that the linear Aboav-Weaire plots found for the cases of the dislocation and vacancy may not be indicators of maximum entropy states.

C. Metrical properties

Various measures of area are broadly in accord with expectation, and with previous results for topological defects [14], and need not be reported in detail. The area of the cluster for all types of point defects and, in the case of the impurity bubbles, the area of the cluster boundary and of the large central bubble increase linearly with the number of bubbles in the cluster (n_c), as might be expected. As for topological defects [14], the average area per bubble in the boundary of the cluster about an impurity bubble, when normalized by the area in an ordered region of the foam at the same age, fluctuates about a constant value $\approx 0.9\pm0.1$.

Simple arguments suggest that the number of sixfold-coordinated cells in the periphery of the cluster should scale as $\pi\sqrt{n_c}$ (to within a numerical factor of order unity). To a good approximation we can take this number to be the total number of sixfold-coordinated cells in the cluster, n_6. For all types of defect studied, n_6 does grow smoothly with n_c (Fig. 14). However, the variation found does not accord with the expected dependence: at low n_c the continuum treatment inherent in the arguments used must break down, there being little area to accommodate internal bubbles, while large clusters tend to develop irregular outlines, increasing the number of bubbles in the 6-belt (there will also be an increased probability of sixfold-coordinated cells internal to the cluster).

D. Multiple dislocations

The results presented above for isolated point defects generally support the conclusions of recent simulations [8,9]. In particular μ_2 increases systematically as the disorder grows around the initial defect; the decreases at large times observed for certain types of defect are caused, we believe, by the nongeneric behavior of threefold-coordinated bubbles and cannot be associated with the decrease in μ_2 from a transient high value observed in the evolution of initially relatively ordered soap froths [3]. To further our understanding of this phenomenon in froths we briefly consider the

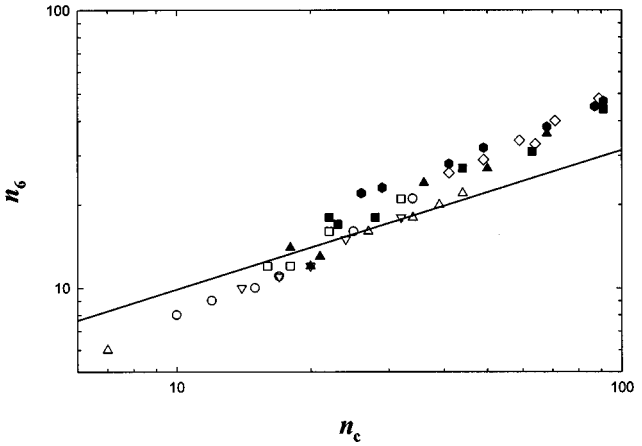

FIG. 14. The variation of n_6, the number of six-coordinated bubbles in the cluster with n_c for different point defects (open symbols) and multiple dislocations (full symbols; see below). The line represents $\pi\sqrt{n_c}$ (see text for discussion).

evolution of disorder about spatially separated defects in an otherwise sixfold-coordinated foam.

The technique used for creating vacancies and bound pairs of dislocations can be adapted to produce multiple dislocations in the foam. Typically we produce two dislocations separated more or less widely along one of the extra half-lines of bubbles (Fig. 15). Bound pairs of dislocations are formed by filling in one of the missing half-lines. However, if the number of bubbles added is m more or less than the number required to complete the extra half layer, a pair of dislocations separated by m bubbles is created. If we add m more bubbles, the two dislocations are joined by a common extra half-line of bubbles (''internal half-line''); if m fewer, there is a common missing half-line (''external half-lines''). As a further complication, in the former case the bubbles forming the cluster may be compactly or noncompactly packed. In all these cases the Burgers vector is always zero, as the extra half-lines cancel each other. We define the cluster here as the set of bubbles around the pair of dislocations having at least one nonhexagonal neighbor, plus the belt of sixfold-coordinated bubbles (two bubbles wide) separating the pair of dislocations.

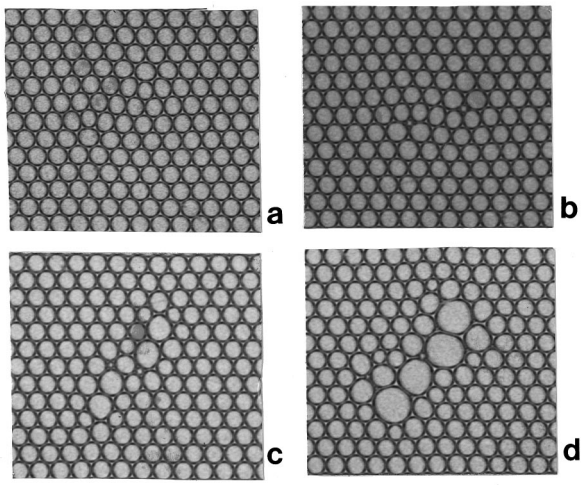

FIG. 15. Pictures of a 2D foam with multiple dislocations. (a) The foam as formed, and for (b) $t=11$, (c) $t=23$, and (d) $t=35$ h.

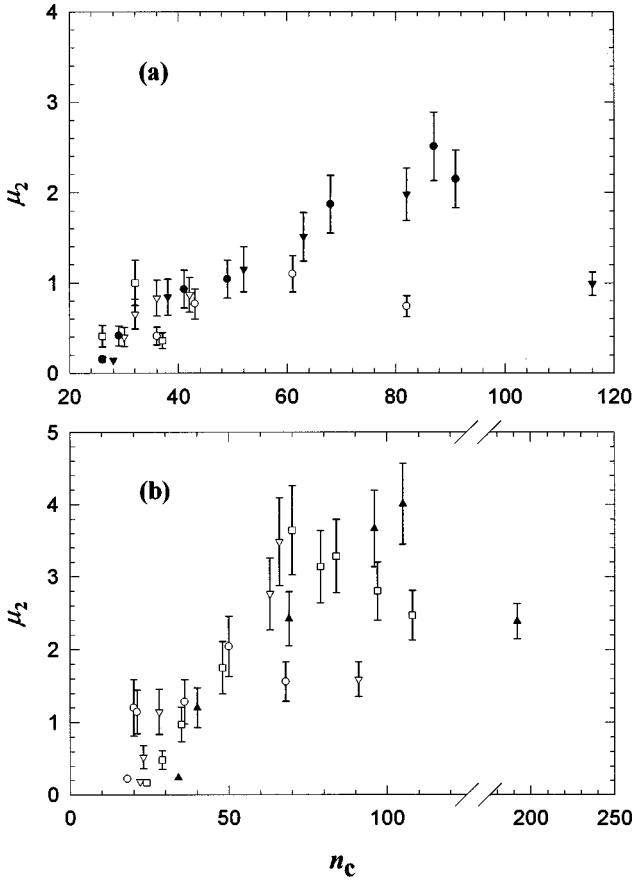

FIG. 16. The variation of μ_2 with n_c for multiple dislocations with $m=4$, having (a) noncompact internal half-line (open symbols) and external half-lines (full symbols); (b) compact internal half-line for $m=2-4$ (open symbols) and for one example with four dislocations and $m=4$ (full symbols).

Figure 16(a) shows the variation of μ_2 with n_c for two dislocations separated by m bubbles (noncompact internal half-line and external half-lines). μ_2 is relatively low compared to that for the bound pair of dislocations (Fig. 8) due to the inclusion of the belt between the dislocations. It reaches higher values for external half-lines compared to internal half-lines. In the former case the regions of disorder around the separate dislocations merge with each other quite early, so that the cluster has time to become very disordered before the experimental cutoff. For internal half-lines the belt of sixfold-coordinated bubbles persists longer. However, the data for both cases show excellent general accord. In the figure two points fall well below the trend; we will discuss these data, which represent the late stages of two different experiments, below.

For compact internal half-lines the compactness of the packing in the cluster leads to thinner liquid walls, allowing faster diffusion of gas between the bubbles than the previous case, so that the bubbles in the cluster evolve more rapidly. μ_2 reaches higher values than for the previous cases before eventually decreasing [Fig. 16(b)].

By perturbing a compact cluster having an internal half-line the number of dislocations can be increased to three or four. However, the behavior of μ_2 remains much as for the original two dislocations. One set of data in Fig. 16(b) represents an experiment in which such a rearrangement of bubbles was induced, creating four dislocations. μ_2 reaches a

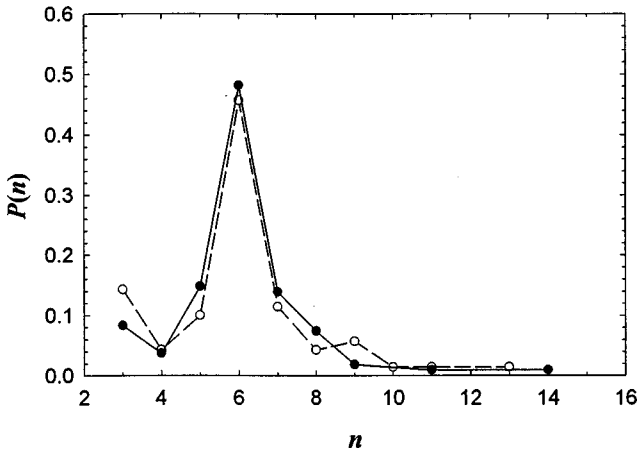

FIG. 17. Topological class distributions for an example of foam containing multiple dislocations [□ in Fig. 16(b)]: at maximum of μ_2 (○) and at final state (●).

rather higher value than for two dislocations but then declines. The large values of μ_2 are only partially due to the presence of threefold-coordinated bubbles, but also reflect significant disorder in the cluster.

In all of these cases a decline in μ_2 occurs. This takes place long after the point at which two ''clusters'' around the individual dislocations merge, which typically happens as μ_2 increases to ≈ 1.2. This merging is followed by a significant growth of μ_2 as the cluster becomes very disordered, before this statistic eventually decreases. Unlike the case of isolated defects the major reason for this decline in μ_2 at long times is not the disappearance of threefold-coordinated bubbles; in some experiments their number actually increases. Threefold-coordinated bubbles do vanish, but their number is replenished from the populations at $n=4$ and 5. The decrease in μ_2 appears to arise from local T_1 rearrangements due to coarsening of the foam. The wings of $P(n)$ decrease, while the central narrow peak, for $5 \leqslant n \leqslant 8$, broadens (Fig. 17): the foam is evolving towards a more generally disordered state.

These observations appear to run counter to a recently suggested explanation [15] of the decrease in μ_2 during the initial transient in foam, which starts out relatively ordered [3]. This involves growth of clusters about point defects randomly distributed in the foam: it is suggested that as the clusters grow into each other they will form a random Voronoi network, having μ_2 appropriate to such a system ($\mu_2 = 1.82$). However, this random network will comprise clusters, not cells, and it is not clear what relation this value of μ_2 would bear to that for the foam. The present data suggest that the decrease in μ_2 found after the initial transient for rather ordered foam may be a natural consequence of the evolution about spatially separated point defects.

IV. CONCLUSIONS

We have investigated the evolution of disorder around single point defects in otherwise ideally sixfold-coordinated bubble rafts, used as model 2D foams. For all types of defect we find that the second moment of the topological class distribution, μ_2, increases with time; the decreases observed at late times in some instances are, we believe, nongeneric, arising from the nature of the model foam used. This conclusion lends some support to certain recent computer simulations [8,9]. However, in the presence of multiple dislocations in the foam the time variation of μ_2 shows a definite peak, which appears to be a real consequence of coarsening in the foam. This observation may be relevant to understanding the transient that has been observed in initially ordered 2D soap froths as they evolve towards a scaling state [3].

It is appropriate to recapitulate upon differences between our experimental system and the computer simulations [8,9] and 2D soap froths [3,4] with which comparisons have been drawn.

(i) The wetness of the foam has been noted at several points. The liquid component leads to specific differences from dry froths, particularly the presence of a significant, rather long-lived population of small threefold-coordinated bubbles. While this leads to a larger μ_2 than for froths, the increases seen may be generic.

(ii) The data extend over relatively short times, due to generalized disorder arising from imperfections of the initial state. Certainly, as shown by our considerations of the topological correlations, our data do not extend to statistical equilibrium, as in the long time limit explored in computer simulations [5,8].

(iii) Largely following from the previous point, our samples of bubbles within the clusters are small, leading to large uncertainties on the data.

These considerations suggest that, as implied earlier, comparisons with dry froths should be treated with some caution.

We have further investigated topological correlations in these systems. Topological correlations found for random 2D foam, such as the Aboav-Weaire law [19,20] and the Lemaître law [21,26], can be derived from maximum entropy arguments, indicating that they relate to systems in statistical equilibrium. Perhaps surprisingly, in some, though not all, cases the area of disordered foam evolving about a point defect yields a linear Aboav-Weaire plot. Unfortunately the statistics of our system are not adequate to check the generic origin of such topological correlations. For all types of defects the plot of μ_2 versus $P(6)$, the probability of sixfold-coordinated bubbles, shows a reasonable collapse to a unique variation, which is, however, very different from that expressed via Lemaître's law. In particular, for a given $P(6)$, the values of μ_2 found here are significantly larger than expected from that law. This is a further consequence of the nature of the model foam used. However, the collapse does indicate that the behavior observed for different defects has a certain generality.

ACKNOWLEDGMENTS

This research was supported by the EPSRC and also in part by the EU HCM Program, Network Contract No. ERBCHRXCT940542. The Irish Centre for Colloid Science and Biomaterials is supported by the International Fund for Ireland. We would like to thank Professor N. Rivier for helpful discussions.

[1] D. Weaire and N. Rivier, Contemp. Phys. **25**, 59 (1984); J. Stavans, Rep. Prog. Phys. **56**, 733 (1993).
[2] J.A. Glazier, S.P. Gross, and J. Stavans, Phys. Rev. A **36**, 306 (1987).
[3] J. Stavans and J.A. Glazier, Phys. Rev. Lett. **62**, 1318 (1989).
[4] J. Stavans, Phys. Rev. A **42**, 5049 (1990).
[5] B. Levitan, Phys. Rev. Lett. **72**, 4057 (1994).
[6] D. Weaire, Phys. Rev. Lett. **74**, 3710 (1995).
[7] C. Sire, Phys. Rev. Lett. **74**, 3708 (1995).
[8] Y. Jiang, M. Mombach, and J.A. Glazier, Phys. Rev. E **52**, 3333 (1995).
[9] H.J. Ruskin and Y. Feng, J. Phys.: Condens. Matter **7**, L553 (1995).
[10] B. Levitan and E. Domany, Phys. Rev. E **54**, 2766 (1996).
[11] J.J. Chae and M. Tabor, Phys. Rev. E **55**, 598 (1997).
[12] M.A. Fortes, M.F. Vas, and D. Grosshans (unpublished).
[13] A. Abd el Kader and J.C. Earnshaw, Philos. Mag. A **76**, 1251 (1997).
[14] A. Abd el Kader and J.C. Earnshaw, Phys. Rev. E **56**, 3251 (1997).
[15] M.F. Vaz and M.A. Fortes, J. Phys.: Condens. Matter **9**, 8921 (1997).
[16] W.L. Bragg and J.F. Nye, Proc. R. Soc. London, Ser. A **190**, 474 (1947).
[17] M.M. Nicolson, Proc. Cambridge Philos. Soc. **45**, 288 (1949).
[18] D. Weaire and M.A. Fortes, Adv. Phys. **43**, 685 (1994).
[19] D.A. Aboav, Metallography **3**, 383 (1970); D. Weaire, *ibid.* **7**, 157 (1974).
[20] N. Rivier, Philos. Mag. B **52**, 795 (1985); Physica D **23**, 129 (1986).
[21] G. Le Caër and R. Delannay, J. Phys. A **26**, 3931 (1993).
[22] C.J. Lambert and D. Weaire, Philos. Mag. B **47**, 445 (1983).
[23] M.A. Peshkin, K.J. Strandburg, and N. Rivier, Phys. Rev. Lett. **67**, 1803 (1991).
[24] F.P. Preparata and M.I. Shamos, *Computational Geometry* (Springer, New York, 1985), Chap. 4.
[25] N. Rivier, J. Phys. I **4**, 127 (1994).
[26] J. Lemaître, A. Gervois, D. Bideau, J.P. Troadec, and M. Ammi, C. R. Acad. Sci. Paris **315**, 35 (1992).
[27] N. Rivier, in *From Statistical Physics to Statistical Inference and Back*, edited by P. Grassberger and J.P. Nadal (Kluwer, Dordrecht, 1994), pp. 77–93.